Analysis of Nonideal Kinetics in the Polymerization of Methyl Methacrylate Using Some Complex Initiator Systems Based on a Pyridine–Sulfur Dioxide Charge Transfer Complex

SAMIR BISWAS

Department of Chemistry and Chemical Technology, Vidyasagar University, Midnapur, West Bengal, India 721102

Received 31 July 1996; accepted 24 March 1997

ABSTRACT: The kinetic nonideality in the polymerization of methyl methacrylate was studied with the use of pyridine–sulfur dioxide charge transfer complex as the initiator under different conditions. The following systems were studied: (1) aqueous polymerization of methyl methacrylate (MMA) with the use of a pyridine–sulfur dioxide charge transfer complex as initiator, (2) photopolymerization of MMA initiated by the pyridine–sulfur dioxide complex in the presence of carbon tetrachloride, (3) photopolymerization of MMA in bulk and in a pyridine-diluted system with pyridine–sulfur dioxide alone and in combination with benzoyl peroxide as a photoinitiator. Polymerization in all these cases proceeded by radical mechanisms. The kinetic parameter k_p^2/k_t for the aqueous system was 3.65 L mol^{-1} s^{-1}, and for nonaqueous systems were 1.27×10^{-2} to 1.40×10^{-2} L mol^{-1} s^{-1}. The monomer exponent and initiator exponent for ideal free radical polymerization systems are 1.0 and 0.5, respectively. In the system studied, the ideal kinetics were followed at specific concentration ranges of both monomer and initiator. At different concentration ranges, the systems behave nonideally. The kinetic nonidealities in monomer exponents, i.e., lower or higher than unity, were explained on the basis of (1) the rate-enhancing effect of different solvents, and (2) a radical generation step by *in situ* initiator monomer complexation reaction. The kinetic nonidealities in initiator exponent were analyzed and interpreted in terms of (1) primary radical termination, and (2) degradative initiator transfer with little reinitiator. Analysis of kinetic data shows that the degradative initiator transfer effect is more prominent in the present systems. © 1998 John Wiley & Sons, Inc. J Appl Polym Sci **67:** 585–595, 1998

INTRODUCTION

Sulfur dioxide readily initiates polymerization of methyl methacrylate (MMA) in a nonaqueous system, particularly on photoactivation; and the effective initiating species is the sulfur dioxide monomer (donor acceptor) complex rather than free sulfur dioxide.[1] Pyridine and sulfur dioxide readily react with each other to form a 1 : 1 pyridine–sulfur dioxide charge transfer complex. This is substantiated by spectral analysis in the ultraviolet (UV) region according to the approach described for complexation between tetrahydrofuran and sulfur dioxide.[2] This article reports the kinetic nonidealities of two kinds of polymerization.

(1) The aqueous polymerization of MMA using pyridine–sulfur dioxide (Py–SO_2) as the initiator. In this system, the range of the concentrations of initiator and monomer used are 4.8×10^{-2} to 0.12×10^{-2} and 15.62×10^{-2} to 10.12×10^{-2} mol L^{-1}, respectively.
(2) The nonaqueous photopolymerization of MMA

Journal of Applied Polymer Science, Vol. 67, 585–595 (1998)
© 1998 John Wiley & Sons, Inc. CCC 0021-8995/98/040585-11

using pyridine–sulfur dioxide complex alone and in a pyridine-diluted system, with the range of [Py–SO_2] being 13.8×10^{-2} to 0.41×10^{-2} mol L^{-1}, and that of [MMA] being 9.2–4.2 mol L^{-1}.

(3) The nonaqueous photopolymerization of MMA using the pyridine–sulfur dioxide complex in the presence of carbon tetrachloride. The range of concentrations of different ingredients are as follows: [Py–SO_2] = 3.18–0.53 mol L^{-1}; [methanol] = 3.30–1.35 mol L^{-1}; [CCl_4] = 0.00–1.60 mol L^{-1}.

(4) The pyridine–sulfur dioxide complex in redox combination with benzoyl peroxide in pyridine-diluted system, in which the ranges of monomer, pyridine–sulfur dioxide, benzoyl peroxide, and pyridine are as follows: [MMA] = 8.4–4.2 mol L^{-1}, [Py–SO_2] = 0.00–36×10^{-2} mol L^{-1}, and [Bz_2O_2] = 0.262×10^{-2} to 11.28×10^{-2} mol L^{-1}.

EXPERIMENTAL PROCEDURE

Purification of Monomer and Solvents

Monomer MMA and solvents were purified by standard procedure.[3]

Preparation of Pyridine–Sulfur Dioxide Complex

5 mL of purified pyridine was taken in a test tube, purged with nitrogen, and cooled to about −5°C. SO_2 gas, purified through a series of Scrubbers, was then gently bubbled through the cooled pyridine until saturation. Excess SO_2 gas was allowed to bubble out of the yellow liquid at room temperature (~ 30°C) with slow stirring. Analysis of the prepared pyridine–SO_2 complex showed 45% SO_2 content (a theoretical complex of 1 : 1 pyridine–SO_2 is 44.75%).

UV Absorption Spectra

The UV spectra of aqueous solutions of pyridine (1.5×10^{-4} mol L^{-1}) and of the Py–SO complex prepared (1.5×10^{-4} mol L^{-1}) are shown in Figure 1(A), curves 1 and 5, respectively (λ_{max} for each spectrum is 257 nm). Aqueous solution of SO_2 (1.5×10^{-4} mol L^{-1}) shows little absorption in the wavelength studied. For a fixed pyridine content (1.5×10^{-4} mol L^{-1}) in water, λ_{max} increases progressively with an increasing proportion of sulfur dioxide added to the system until the latter is used in equimolar proportion [(1.5×10^{-4} mol L^{-1}); see Fig. 1(A)]; with a further increase in SO_2 content, no further changes in the absorption spectra are visible. None of the spectra in Figure 1(A) changed with time.

In two separate sets of experiments, absorption values at λ_{max} for solutions of pyridine and Py–SO_2 complex in water at several concentrations were determined, and the data were plotted as in Figure 1(B). In each case, the plot passing through the origin is linear, with the Py–SO_2 plot giving a higher slope than the pyridine plot. The overall absorbance at λ_{max} (257 nm) for each of various mixtures of pyridine and SO_2 [Fig. 1(A)] is equal to the summation of the absorbances corresponding to the calculated amount of 1 : 1 Py–SO_2 complex in the system and that of pyridine present in excess of SO_2 on a mole-to-mole basis. As expected, excess SO_2 where ever present, has little influence on the overall absorbance. Thus, it is clearly indicated that the complexation between pyridine and SO_2 takes place almost instantly, and the complex has a 1 : 1 composition.

The 1 : 1 nature of the prepared Py–SO_2 complex was further substantiated by spectral analysis in the UV region in CCl_4 solution. The results of the spectral studies are given in Figure 1(C) and (D). UV absorption spectra of the Py–SO_2 complex in MMA (MMA in the reference cell) is given in Figure 1(E); λ_{max} at 295 nm clearly indicates the complexation of MMA with the Py–SO_2 complex.

POLYMERIZATION PROCEDURE

Two types of polymerization experiments were carried at 40°C: (1) thermal polymerization of MMA in an aqueous media using the Py–SO_2 complex; and (2) photoinitiated polymerization of MMA in the presence of organic solvents and other additives.

Thermal Polymerization of MMA in Aqueous Media

Aqueous polymerization of MMA was carried out in a 150 mL stoppered conical flask under nitrogen following the usual procedure.[4,5] The initial monomer content was usually 1.5% *V/V*. The monomer was allowed to dissolve in the aqueous media under a blanket of nitrogen for about 20 h before the addition of the initiator. Most of the experiments were carried out at 40°C. Rate mea-

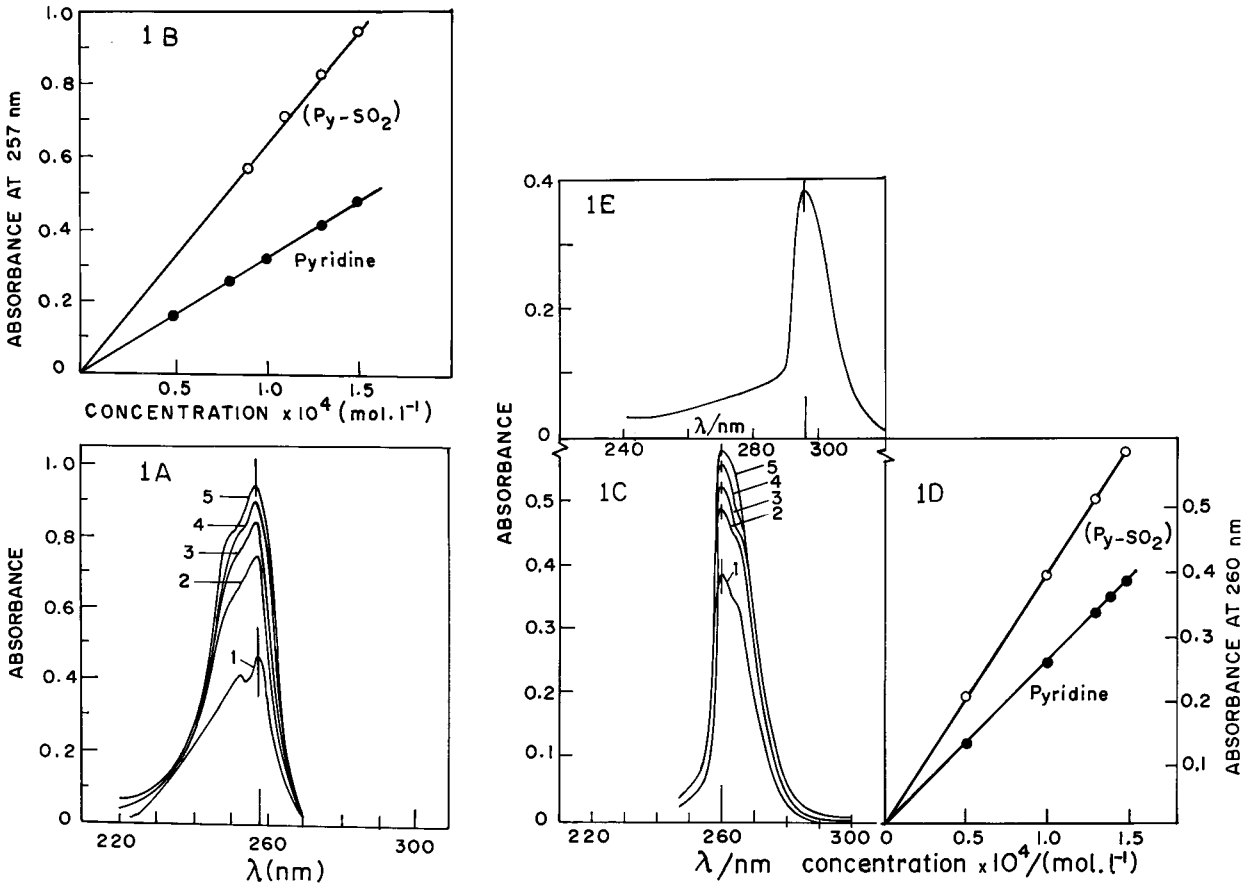

Figure 1 (A) UV absorption spectra of SO_2, the Py–SO_2 complex, and different mixtures of SO_2 and pyridine in aqueous solution: (1) pyridine = 1.5×10^{-4} mol L^{-1}, (2) pyridine = 1.50×10^{-4} mol L^{-1} and SO_2 = 0.90×10^{-4} mol L^{-1}, (3) pyridine = 1.50×10^{-4} mol L^{-1} and SO_2 = 1.1×10^{-1} mol L^{-1}, (4) pyridine = 1.50×10^{-1} mol L^{-1} and SO_2 = 1.30×10^{-4} mol L^{-1}, and (5) pyridine = 1.50×10^{-4} mol L^{-1} and SO_2 = 1.50×10^{-4} mol L^{-1}. (B) Plot of absorbance at 257 nm versus concentration for pyridine and the Py–SO_2 complex, each in a water solution (water in the reference cell). (C) UV absorption spectra of pyridine, Py–SO_2 complex, and different mixtures of pyridine and SO_2 in a CCl_4 solution using CCl_4 as a reference in each case. (1) [Py] = 1.5×10^{-4} mol L^{-1}; [SO_2] = 0×10^{-4} mol L^{-1}; (2) [Py] = 1.5×10^{-4} mol L^{-1}; [SO_2] = 0.75×10^{-4} mol L^{-1}; (3) [Py] = 1.5×10^{-4} mol L^{-1}; [SO_2] = 1.00×10^{-4} mol L^{-1}; (4) [Py] = 1.5×10^{-4} mol L^{-1}; [SO_2] = 1.25×10^{-4} mol L^{-1}; (5) [Py] = 1.5×10^{-4} mol L^{-1}; [SO_2] = 1.5×10^{-4} mol L^{-1}. (D) Plot of the absorbance at 260 nm versus the concentration of pyridine and the Py–SO_2 complex, each in CCl_4 solution (CCl_4 in the reference cell). (E) UV absorption spectra of the Py–SO_2 complex (1M mol L^{-1}) in MMA (MMA in the reference cell).

surements were done following standard procedure [5].

Photopolymerization experiments were carried out in corning dilatometer using a constant temperature bath made of borosil glass and controlled to ±0.5°C. A high-pressure 125 W mercury vapor lamp (Philips India Ltd., Calcutta), having appreciable intensities near the 440 and 570 nm wavelength region, was used as the light source. The light intensity was controlled through a suitable power supply system. The various kinetic parameters were determined according to the usual procedure.[6] Polymers at low conversions (<10%) were removed from dilatometers and were isolated by precipitation with petroleum ether and drying in vacuum at 50°C. The degree of polymerization ($\bar{P}_n$) and molecular weight ($\bar{M}_m$) of selected polymers were determined viscometrically

Table I Rates of Photopolymerisation of MMA at a Constant Monomer Concentration [*M*] = 5.0 mol L^{-1} and at Varying Concentrations of Pyridine (Py) Using a Fixed Concentration of Bz_2O_2 (2.24×10^{-2} mol L^{-1}) and Py–SO_2 (3.63×10^{-2} mol L^{-1}) at 40°C[a]

Volume of Pyridine (mL)	Volume of Benzene (mL)	Inhibition Period (min)	$R_p = 10^5$ (mL L^{-1} s^{-1})	[Py] (mL L^{-1})	[*n*] (di g)
0	5	79	7.26	0	1.22
1	4	61	7.76	1.127	1.08
2	3	55	10.43	2.254	0.88
3	2	37	12.84	3.381	0.72
4	1	20	13.91	4.510	0.72
5	0	4	18.55	5.630	0.68

[a] Requisitive volume of benzene was used as an inert balancing solvent.

using benzene as the solvent at 30°C following the usual procedure.[7]

RESULTS AND DISCUSSION

The aqueous polymerization of MMA initiated by the Py–SO_2 complex at 40°C was associated with a inhibition period (IP) of 5–15 min for the initiator concentration ranges of 4.8×10^{-2} to 0.12×10^{-2} mol L^{-1}. In general, higher [Py–SO_2] gives lower IP.

Nonaqueous bulk photopolymerization of the Py–SO_2 complex in the concentration range of 1×10^{-3} to 200×10^{-3} mol L^{-1} showed inhibition period of 160–80 min. As the Py–SO_2 complex is not miscible with MMA when used in concentrations 0.2 mol L^{-1}, a known quantity of methanol is used to make them homogeneous. In the presence of 2–3% CCl_4, the IP is greatly reduced. IP is practically zero when [CCl_4] $\geq$ 0.1 mol L^{-1}.

In the photopolymerization using the combination of benzoyl peroxide (Bz_2O_2) the Py–SO_2 complex as the initiator in the pyridine media, pyridine acts as a rate-enhancing solvent. The rate-enhancing role of pyridine[8] is shown in Table I, giving R_p and inhibition periods at a fixed monomer concentration, [*M*], and at varied pyridine concentration, [Py], employing the combination of benzoyl peroxide and Py–SO_2 complex as the photoinitiator.

Initial rates of polymerization were significantly higher when the combination of Bz_2O_2 and the Py–SO_2 complex was used than when either of them was used alone as the photoinitiator.

Rates of polymerization (R_p) were calculated for all systems from the slopes of the initial linear zones of the percentage of conversion versus time plots.

Monomer Exponent and Initiator Exponent

For the aqueous polymerization system, a plot of log R_p versus log[Py–SO_2] indicates that the initiator exponent is 0.5 for [Py–SO_2] $\leq$ 0.02 mol L^{-1}. For [Py–SO_2] $>$ 0.02 mol L^{-1}, the initiator exponent is practically zero (See Figure 2, Table II).

At fixed [Py–SO_2] $<$ 0.02 mol L^{-1}, the monomer exponent obtained from the slope of the plot of log

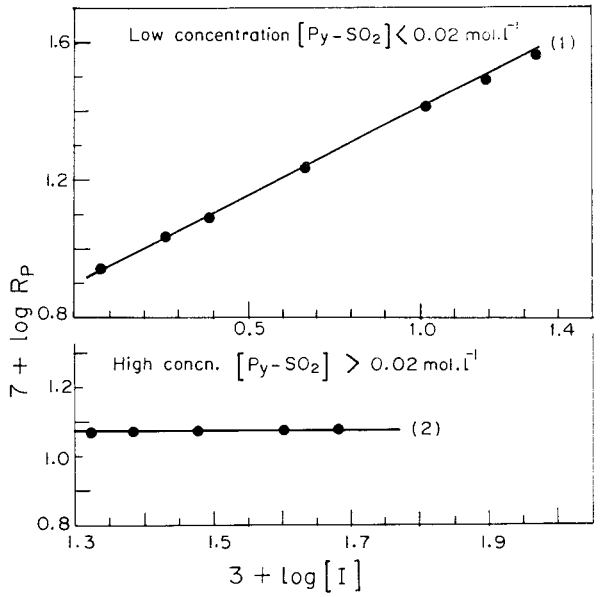

Figure 2 Aqueous polymerization of MMA at 40°C using Py–SO_2 as the initiator. Plot of log R_p versus log[*I*]: (1) at low [Py–SO_2] $\leq$ 0.02 mol L^{-1}; and (2) at high [Py–SO_2] $>$ 0.02 mol L^{-1}.

Table II Aqueous Polymerization of MMA at 40°C Using the Py–SO_2 Complex as an Initiator, with Variation of R_p with the Initiator Concentration[a]

Py–SO_2 × 10^3 mol L^{-1}	R_p × 10^7 mol L^{-1} s^{-2}	n di g	Initiator Exponent	k_p^2/k_t L mol^{-1} s^{-2}
1.20	8.60	4.88		
1.80	10.90	4.65		
2.40	12.00	4.33	0.50	
4.80	17.32	3.88		
10.80	24.15	2.77		
15.20	30.40	2.28		
				3.66
21.00	36.00	2.02		
24.00	37.00	1.98		
32.00	37.00	1.95	0.00	
40.00	37.00	1.93		
48.00	37.00	1.92		

[a] $[M] = 13.85 \times 10^{-2}$ mol L^{-1}.

R_p versus log[m] is 1.5 (Fig. 2). If [Py–SO_2] > 0.02, the monomer exponent is 1.00 (Fig. 3).

The bulk polymerization of MMA using the Py–SO_2 complex (1×10^{-3} to 200×10^{-3} mol L^{-1}) as the photoinitiator at 40°C shows that the initiator exponent is 0.3 (Fig. 4). The monomer exponent obtained from the slope of the plot of log R_p versus log[M] in the pyridine-diluted system is 1.00 (Fig. 5).

The Py–SO_2 complex is not quite miscible with MMA when used in concentrations > 0.2 mol L^{-1}. Some quantities of methanol, a polar solvent, is used to make them soluble. In the presence of 2–3% CCl_4 (0.2–0.3 mol L^{-1}), the rate of polymerization (R_p) is greatly enhanced. Almost instanteneous polymerization was observed, even with low [CCl_4] < 0.05%, while there was usually an inhibition period (30–60 min) in systems containing no CCl_4. At low [CCl_4], R_p is dependent on both [CCl_4] and [Py–SO_2]. The [Py–SO_2] ex-

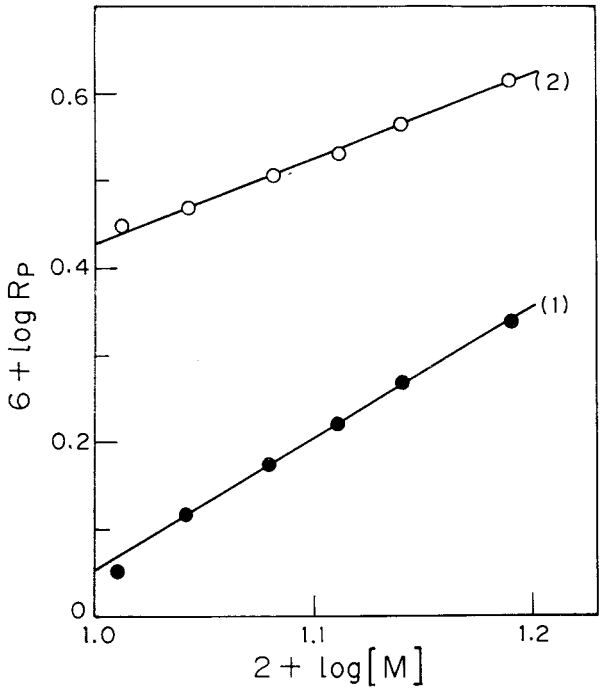

Figure 3 Aqueous polymerization of MMA at 40°C using the Py–SO complex as the initiator at different concentrations of MMA. Plot of log R_p versus log[M]: (1) [Py–SO_2] = 5.50×10^{-3} mol L^{-1}; and (2) [Py–SO_2] = 32.00×10^{-3} mol L^{-1}.

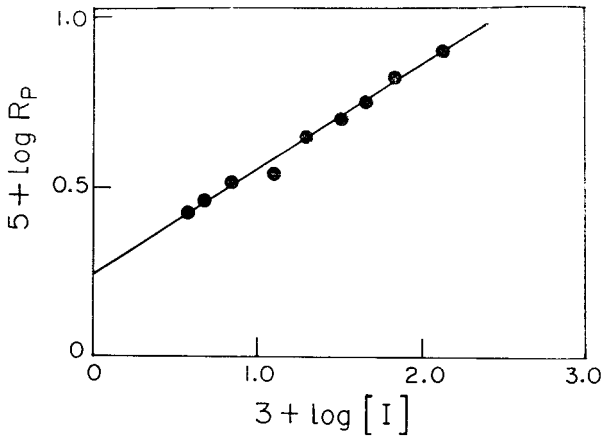

Figure 4 Photopolymerization of MMA (bulk) using the Py–SO complex as the initiator (I) at 40°C. Plot of log R_p versus log[I].

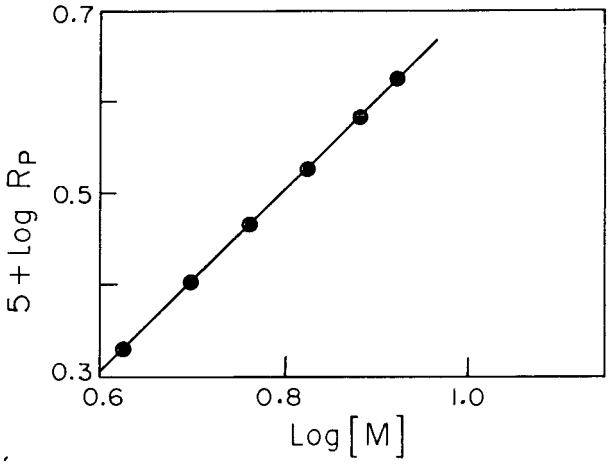

Figure 5 Photopolymerization of MMA using the Py–SO_2 complex as the initiator at 40°C. Plot of log R versus log[M].

ponent was calculated from the slope of the plot of log R_p versus log[Py–SO_2] at a fixed [CCl_4] and [M] [Fig. 6(A)]. The [CCl_4] exponent was calculated from the slope of the plot of log R_p versus log[CCl_4] at a fixed [Py–SO_2] and [M]. In this study, [Py–SO_2] used was high (0.5–3.2 mol L^{-1}). [CCl_4] ranged between 0 and 1.5 mol L^{-1}. At a fixed [Py–SO_2] and [M], the CCl_4 exponent is 0.5 for [CCl_4] $<$ 0.01 mol L^{-1}, and it is independent of [CCl_4] when [CCl_4] $>$ 0.5 mol L^{-1} [Fig. 6(B)].

Variation of R_p with monomer concentration in toluene and methanol diluted system is shown in the form of log R_p versus log[M] (Fig. 7), the slope of each plot giving a monomer exponent of 1.5.

The monomer and initiator exponent of the polymerization of MMA using the Bz_2O_2 and Py–SO_2 redox system were also studied. Rates of photopolymerization at a fixed dilution with pyridine at various concentrations of Bz_2O_2 for a fixed concentration of Py–SO_2 complex and vice versa were measured, and the results are given in Figure 8. Examination of data indicates that the reaction order with respect to benzoyl peroxide follows an interesting pattern; the order is 0.5 (normal kinetics), when the mole ratio of [Bz_2O_2] : [Py–SO_2] is greater than or equal to 1, and the order is significantly less than 0.5 (0.1–0.2) when the molar ratio [Bz_2O_2] : [Py–SO_2] is less than 1 (nonideal kinetics). This pattern is followed over the whole range of dilution with [Py] = 1.12–6.7 mol L^{-1}. Similarly, the order of overall polymerization with respect to Py–SO_2 complex at one fixed dilution level ([Py] = 1.13 mol L^{-1}) is 0.5 when [Py–SO_2] : [Bz_2O_2] is greater than or equal to 1 and significantly less than 0.5 (observed value is 0.2) when [Py–SO_2] : [Bz_2O_2] is less than or equal to 1.

The rates of photopolymerization were then determined in several sets of experiments using a fixed concentration of the Py–SO_2 complex; in each set, the monomer concentration was varied, using different proportions of pyridine solvent and keeping benzoyl peroxide concentration fixed. The concentration of Bz_2O_2 was different, however, in different sets of experiments. Log R_p versus log[M] plots for the different sets are given in Figure 9(A) and (B). The monomer exponent clearly appears to depend on [Bz_2O_2], with the

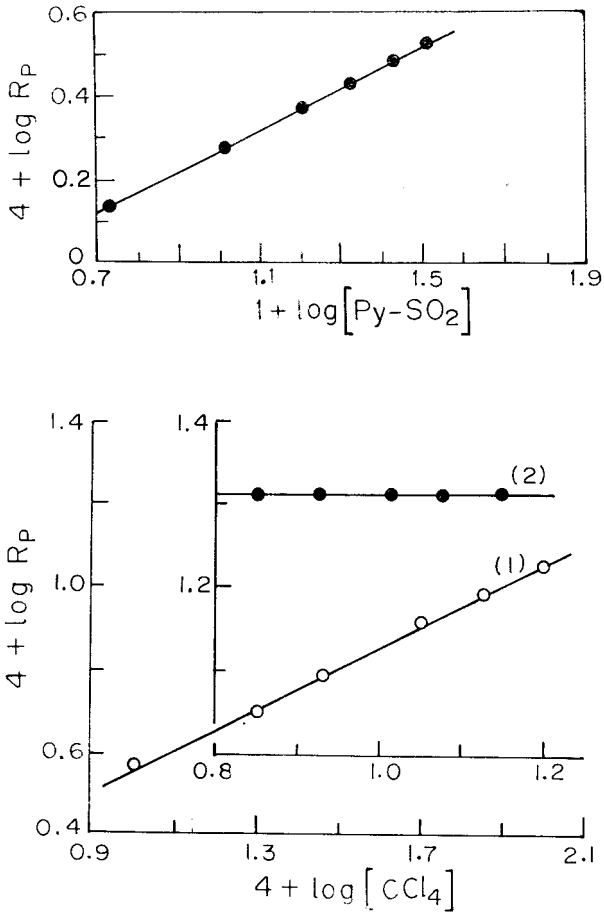

Figure 6 (A) Photopolymerization of MMA using the Py–SO_2 complex (I) as the initiator in the presence of CCl_4 at 40°C. Plot of log R_p versus log[I]: CCl_4 = 0.689 mol L^{-1} (fixed); [M] = 3.68 mol L^{-1} (fixed). (B) Photopolymerization of MMA using the Py–SO_2 complex as the initiator in the presence of CCl_4 at 40°C. Plot of log R_p versus log[CCl_4]: [M] = 3.68 mol L^{-1} (fixed), [Py–SO] = 1.59 mol L^{-1} (fixed): (1) at [CCl_4] $\leq$ 0.01 mol L^{-1}; (2) at [CCl_4] $\geq$ 0.70 mol L^{-1}.

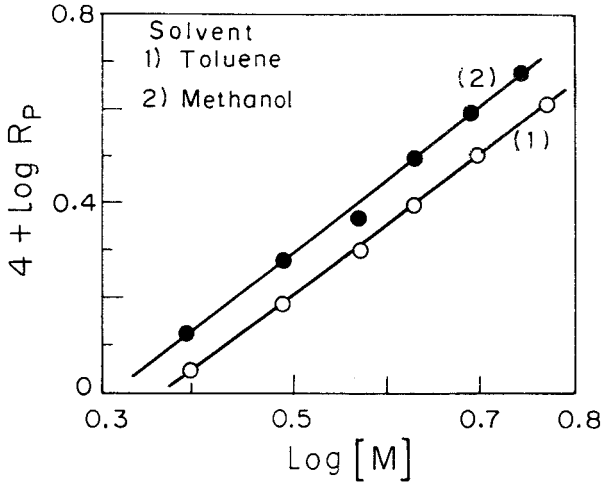

Figure 7 Photopolymerization of MMA using the Py–SO complex as the initiator in the presence of CCl_4 at 40°C. Plot of log R_p versus log[M]: [Py–SO_2] = 1.59 mol L^{-1} (fixed); [CCl_4] = 0.69 mol L^{-1} (fixed); solvent (1) is toluene; solvent (2) is methanol.

value of the exponent becoming progressively lower with higher [Bz_2O_2]; at zero [Bz_2O_2], the monomer exponent is unity, while it is as low as 0.56 when [Bz_2O_2] is 11.28×10^{-2} [M]. This kinetic, nonideality, arises due to the rate-enhancing role of pyridine in the presence of benzoyl peroxide.[8]

Application of the dye partition test of Palit et al.[9] indicated the incorporation of anionic sulfoxy and groups in all the polymers.

MECHANISM

Kinetic data, the presence of sulfoxy and group in the polymers prepared, indicate a radical mechanism.

Normal free radical polymerization kinetics predicts that the initiator and monomer exponent should be 0.5 and 1.0, respectively. The kinetic nonideality of the Py–SO_2 aqueous and Py–SO_2 bulk polymerization systems can be explained on the basis of monomer-dependent initiation and initiator-dependent termination processes. The radical generation step may be described as follows[10]:

$$\text{Py–SO}_2 + M \overset{K}{\rightleftharpoons} [\text{Py–SO}\cdots M] \overset{k_d}{\rightarrow} \text{Pair of radicals} \quad (1)$$

Initiating Complex, I

Assuming bimolecular termination, the rate of polymerization can be expressed as

$$R_p = \left(\frac{k_p^2}{k_t}\right)(fk_dK)^{0.5}[\text{Py–SO}_2]^{0.5}[M]^{1.5} \quad (2)$$

The radical generation process is considered to proceed by a complexation reaction between the monomer and the Py–SO_2 complex molecules, which is characterized by an equilibrium constant K, such that the initiator concentration of the actual initiating complex [I] is given by [I] = K[Py–SO_2][M], and f, k_p, k_d, k_t have their usual significance. The above expression explains well the kinetic nonideality in the monomer exponent, when [Py–SO_2] $< 2 \times 10^{-2}$ mol L^{-1}. The monomer order and initiator order of unity and zero, respectively, for the aqueous polymerization system when [Py–SO_2] $> 2 \times 10^{-2}$ mol L^{-1} may be explained by some initiator-dependent termination processes. The reaction scheme for the pres-

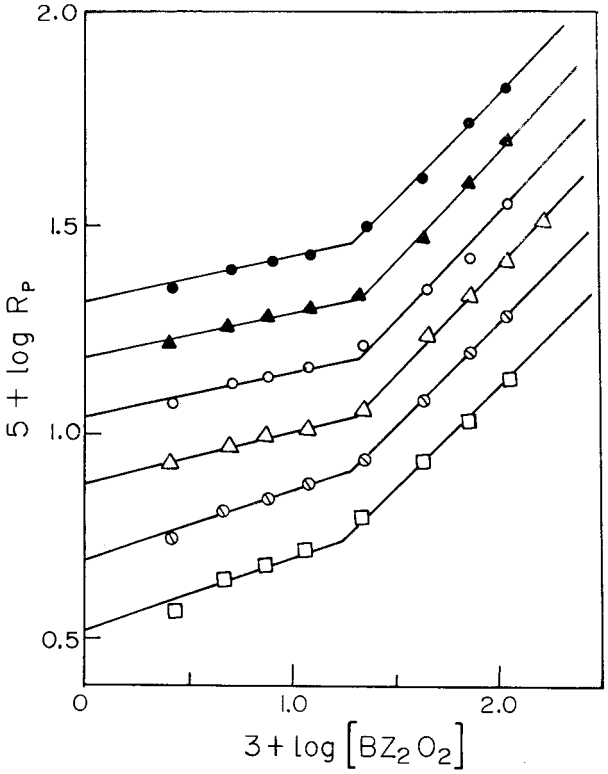

Figure 8 Photopolymerization of MMA using a Bz_2O_2—Py–SO_2 combination as the initiator at 40°C. Plot of log R_p versus log[Bz_2O_2]; [Py–SO_2] = 1.81×10^{-2} mol L^{-1} (fixed). For each curve, data given are [M] in mol L^{-1}: ◒, 4.2; ⊙, 5.0; ◐, 5.88; ○, 6.7; ◑, 7.58; ●, 8.40.

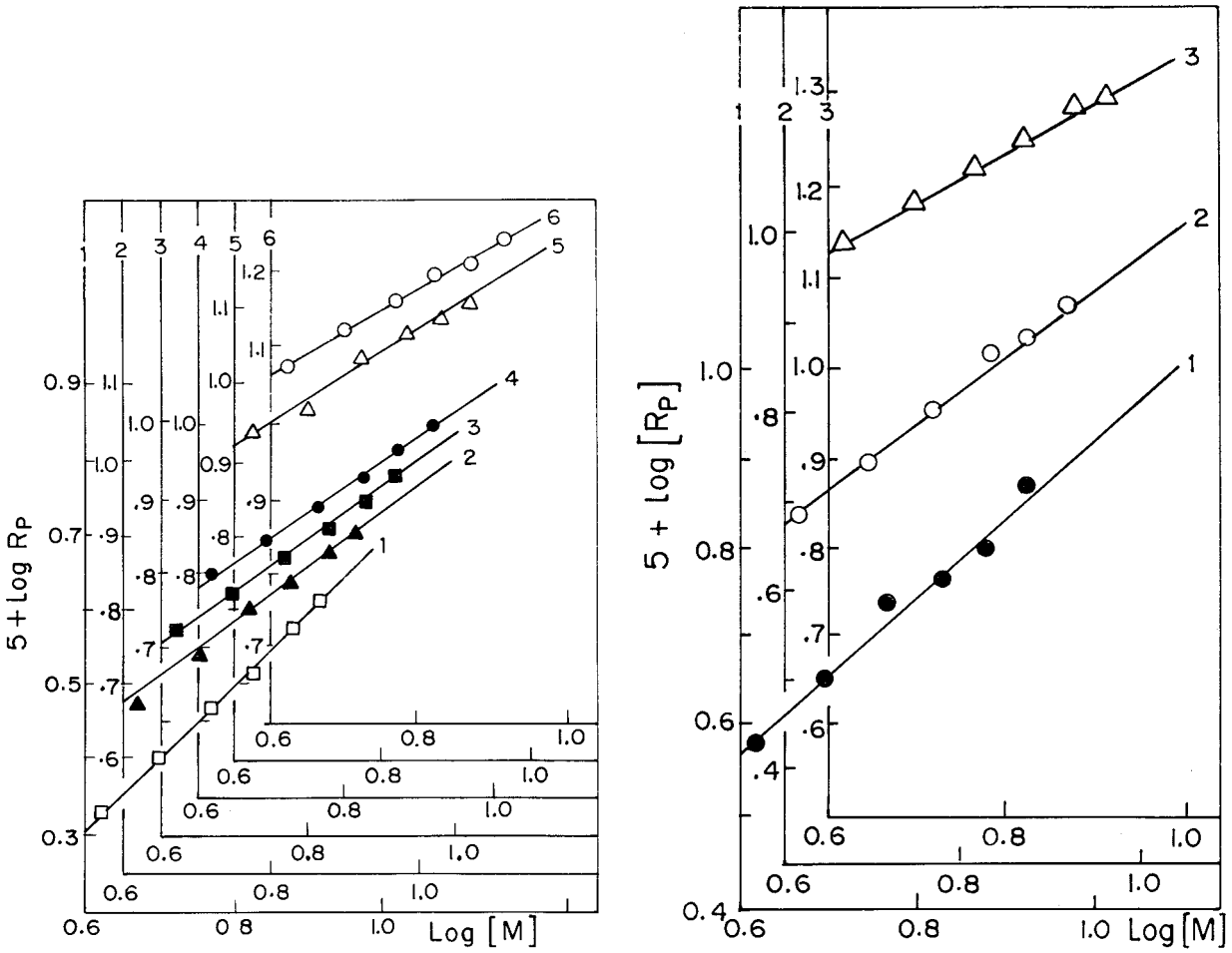

Figure 9 (A) and (B) Photopolymerization of MMA in pyridine using a Bz_2O_2—Py–SO_2 combination as the initiator at 40°C. Plot of log R_p versus log[M]. Py–SO_2 = 1.81 mol L^{-1} (fixed). For each curve, data given are [Bz_2O_2] in mol L^{-1}. (A) ◑, 0.0; ▲, 0.480 × 10^{-2}; ◆, 1.12 × 10^{-2}; ●, 2.24 × 10^{-2}; ⊙, 4.36 × 10^{-2}; ○, 7.43 × 10^{-2}. (B) ●, 0.262 × 10^{-2}; ⊙, 0.75 × 10^{-2}; ◑, 11.28 × 10^{-2}.

ent polymerization when [Py–SO_2] > 2 × 10^{-2} mol L^{-1} may be written as follows:

$$I \xrightarrow{k_d} 2R^{\bullet} \qquad R^{\bullet} + M \xrightarrow{k_i} M^{\bullet}$$

$$M^{\bullet} + M \xrightarrow{k_p} M^{\bullet} + I \xrightarrow{k_{tr,I}}$$

polymer + radicals with little or no activity

In this reaction scheme, it is assumed that the termination step is an exclusively degradative initiator transfer with little or no radical activity. Applying steady-state assumption in $R^{\bullet}$ and $M^{\bullet}$, the following equation is obtained:

$$R_p = \frac{2fk_dk_p}{k_{tr,I}}[M] \tag{3}$$

If it is assumed that the termination step is exclusively primary radical with the initiator, the reaction may be written as

$$M^{\bullet} + R^{\bullet} \xrightarrow{k_{prt}} \text{polymer}$$

Steady-state assumption in R and M gives

$$R_p = \frac{k_ik_p}{k_{prt}}[M]^2 \tag{4}$$

The observed monomer exponent of 1.0 and the initiator exponent of 0.0 predicts that the termination occurs exclusively by degradative initiator transfer, with little reinitiation at Py–SO_2 > 2.0 × 10^{-2} mol L^{-1}.

In the bulk photopolymerization system, the

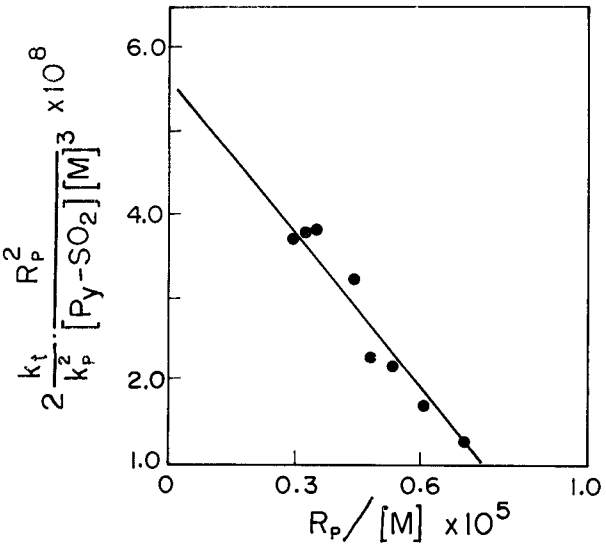

Figure 10 Photopolymerization of MMA (bulk) using the $Py-SO_2$ complex as the initiator as 40°C. Analysis of degradative initiator transfer (no reinitiation effect) from the plot of

$$2\frac{k_t}{k_p^2}\frac{R_p^2}{[\text{Py}-\text{SO}][M]^3} \text{ versus } \frac{R_p}{[M]}.$$

observed $Py-SO_2$ exponent of 0.3 for the entire $[Py-SO_2]$ range (4×10^{-3} to 138×10^{-3} mol L^{-1}) indicates that some kind of initiator-dependent termination process is significant, along with the usual mode of bimolecular termination. The monomer exponent of 1.0 in the pyridine solvent shows that the initiator-dependent termination is an exclusively degradative initiator transfer with little reinitiation in nature. The termination steps in this case may be written as

$$M^\bullet + I \xrightarrow{k_{tr,I}} \text{polymer} + \text{inactive radicals}$$

$$M^\bullet + M^\bullet \xrightarrow{k_t} \text{polymer product}$$

Steady-state assumption in $R^\bullet$ and $M^\bullet$ give the following equation:

$$\frac{2k_t}{k_p^2}\cdot\frac{R_p^2}{[M][\text{Py}-\text{SO}_2]} = 2fk_dK - \frac{k_{tr,I}k}{k_p}\cdot\frac{R_p}{[M]} \quad (5)$$

A plot of left-hand side of the above equation against $R_p/[M]$ (Fig. 10) gives a straight line with a negative slope, the value of $(k_{tr,I}K)/(k_p)$ is 6.133 $\times$ 10^{-5}. For a fixed $[Py-SO_2]$ and $[M]$, R_p increases sharply with an increase in $[CCl_4]$ up to about 0.03 mol L^{-1}; for higher $[CCl_4]$, R_p remains practically independent of $[CCl_4]$. The $[CCl_4]$ exponent changes from nearly 0.5 in a low $[CCl_4]$ range (<0.02 mol L^{-1}) to practically zero in a high $[CCl_4]$ range (>0.2 mol L^{-1}) (Fig. 11). In the CCl_4-activated systems, R_p is proportional to $[Py-SO_2]^{0.5}$ and to $[CCl_4]^{0.5}$ and $[CCl_4]^0$ in a low or high concentration of CCl_4, respectively (Fig. 6). This kinetic nonideality can be explained by the following reaction scheme.

$$Py-SO_2 + M \overset{k_1}{\rightleftharpoons} [Py-SO_2\cdots M] \quad (6)$$

$$I + CCl_4 \xrightarrow{k_3} Cl_3CM + \odot^{N:} + SO_2Cl \quad (7)$$

Assuming bimolecular termination, the rate of polymerization R_p in the presence of CCl_4 may be expressed as

$$R = \left(\frac{k_p^2}{k_t}\right)^{0.5}\cdot k_1^{0.5}[M]^{1.5} \times [\text{Py}-\text{SO}_2]^{0.5}\left(\frac{[CCl_4]}{k_2/k_3 + [CCl_4]}\right)^{0.5} \quad (8)$$

provided there is no polymerization at 40°C in the absence of CCl_4. It is found experimentally that there is no polymerization for the $Py-SO_2$ bulk system within 30 min, whereas the CCl_4-activated photopolymerization is complete within 30 min. In eq. (8), when $[CCl_4] \ll k_2/k_3$, $k_2/k_3 + [CCl_4]$

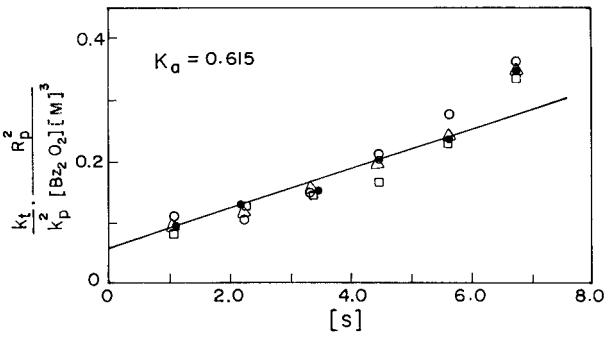

Figure 11 Photopolymerization of MMA in pyridine using the BzO—Py–SO combination as the initiator at 40°C. Determination of k from the plot of $\frac{k_tR_p^2}{k_p^2[Bz_2O_2][M]^3}$ versus $[S]$ (pyridine), where $[Py-SO_2]$ = 1.81×10^{-2} mol L^{-1} (fixed). Data given are $[Bz_2O_2]$ in mol L^{-1}: ⊙, Bz_2O_2, 2.24×10^{-2}; ●, Bz_2O_2, 4.36×10^{-2}; △, Bz_2O_2, 7.43×10^{-2}; ○, Bz_2O_2, 11.28×10^{-2}.

Table III Effect of CCl_4 on R_p in the Photopolymerization of MMA Using the Py–SO_2 Complex as a Photoinitiator at 40°C[a]

CCl_4 (mol L^{-1})	$R_p \times 10^4$ (mol L^{-1} s^{-1})	$[CCl_4]$ (mol L^{-1})	$R_p \times 10^4$ (mol L^{-1} s^{-1})
1.40	2.1	0.34	2.00
1.22	2.1	0.22	1.98
1.04	2.09	0.14	1.97
0.83	2.083	0.069	1.86
0.71	2.060	0.034	1.70
0.55	0.045	0.017	1.47
		0.000	0.137

[a] $[M] = 3.68$ mol L^{-1}; $[Py–So_2] = 1.59$ mol L^{-1}.

$\simeq k_2/k_3$; and the expression for R_p takes the following form:

$$R = \left(\frac{k_p^2}{k_t}\right)^{0.5}\left(\frac{k_1k_3}{k_2}\right)^{0.5}[M]^{1.5}[\text{Py–SO}_2]^{0.5}[\text{CCl}_4]^{0.5} \quad (9)$$

The equation predicts that at low $[CCl_4]$, the CCl_4 exponent and Py–SO_2 exponent both are 0.5, as observed experimentally when $[CCl_4] < 0.01\,[M]$. At a high concentration of CCl_4, $[CCl_4] \gg k_2k_3$, and $k_2k_3 + [CCl_4] \simeq [CCl_4]$, and eq. (8) takes the following form:

$$R = \left(\frac{k_p^2}{k_t}\right)^{0.5} k_1^{0.5}[M]^{1.5}[\text{Py–SO}_2]^{0.5}$$

This equation predicts that the Py–SO_2 exponent is 0.5 and the rate is independent of $[CCl_4]$ at high $[CCl_4]$($[CCl_4] > 0.5$ mol L^{-1}). The observed $[CCl_4]$ exponent is practically zero, as expected.

For high $[CCl_4]$, the value of k_1 was calculated using $[Py–SO_2]$, $[M]$ and taking $k_p^2/k_t = 1.40 \times 10^{-2}$ L mol^{-1} s^{-1}. The calculated value of k_1 is 3.47×10^{-8} L mol^{-1} s^{-1}. Now with the knowledge of k_p/k_t, $[M]$, and $[Py–SO_2]$, and from various values of R_p at different $[CCl_4]$ for $[CCl_4] < 0.1$ mol L^{-1}, the value of the parameter is 0.021 mol L^{-1}.

Photopolymerization in the pyridine-diluted system using the combination of Bz_2O_2 and Py–SO_2 complex as an initiator is characterized by (1) a variable monomer order depending on $[Bz_2O_2]$; (2) a variable Bz_2O_2 order (equal to or less than 0.5), depending on the ratio of Bz_2O_2 : $[Py–SO_2]$; and (3) solvent (pyridine, S) participation in the initiation step, enhancing R_i, the rate of initiation; and (4) reasonable constancy of the apparent value of the parameter k_p^2/k_t(1.4×10^{-2} L mol^{-1} s^{-1} for all levels of dilution at 40°C. The radical generation step in this system is described as

$$\text{Bz}_2\text{O}_2 + \underset{I_1}{[\text{Py–SO}\cdots M]} \xrightarrow{\text{fast}} \underset{I_2}{[\text{Bz}_2\text{O}_2\cdots\text{Py–SO}_2\cdots M]} \xrightarrow{k_d} \text{pair of radicals } (R) \quad (11)$$

In the presence of pyridine (S), an additional radical generation process will be

$$I_2 + S \overset{k_{ds}}{\rightleftharpoons} \text{pair of radicals } (R^\bullet) \quad (12)$$

For $[Bz_2O_2] > [Py–SO_2]$, termination proceeds by the normal bimolecular mechanism; and for $[Bz_2O_2] < [Py–SO_2]$, termination by a degradative initiator transfer with little reinitiation effect are significant additional features.

Assuming no reinitiation following the degradative initiator transfer reaction involving $M^\bullet$ and I_2, the following equation may be deduced with the help of the concept described in this article:

$$\frac{2k_tR_p^2}{k_p^2[\text{Bz}_2\text{O}_2][\text{Py–SO}_2][M](1 + k_a[S])} = 2fk_dK - \frac{k_{tr,I}KR_p}{k[M](1 + K[S])} \quad (13)$$

where $K_a = f_sk_{ds}/fk_d$ for the analysis of the kinetic data for a fixed value of $[Py–SO_2]$ corresponding to those given in Figure 8. Evaluation of the constant K_a is necessary under the condition of purely bimolecular termination corresponding to a Bz_2O_2 order 0.5; the initiator-dependent termination processes are negligible or nonexistent. Equation (13) reduces to

$$\frac{k_tR_p^2}{k_p^2[\text{Bz}_2\text{O}_2][M]^3} = 2fk_d[\text{Py–SO}_2]k + 2fk_dKK_a[\text{Py–SO}_2][S] \quad (14)$$

A plot of the left-hand side of eq. (14) would be expected to be linear, and the ratio of the slope to

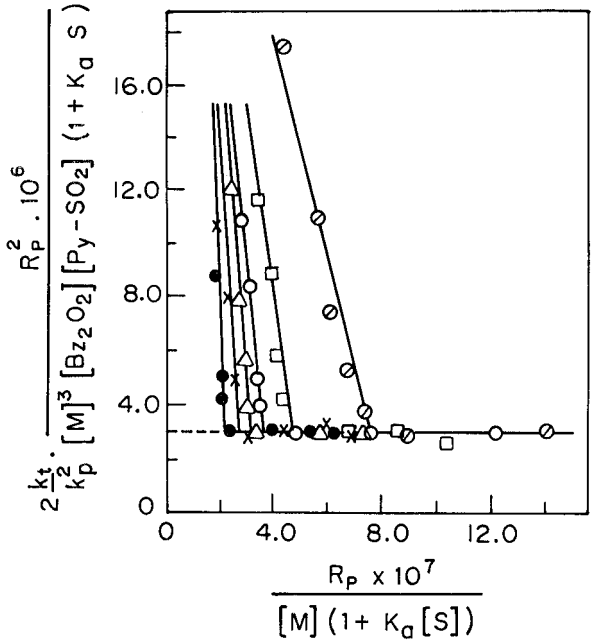

Figure 12 Analysis of the degradative initiator transfer and its variation of the concentration of pyridine (S) in the photopolymerization of MMA using the Bz_2O_2—Py–SO_2 combination as the redox initiator at 40°C. Plot of $\left[\frac{2k_t}{k_p^2}\frac{R_p^2}{[M][Bz_2O_2][Py-SO_2](1+k_a[S])}\right]$ versus $\frac{R_p}{[M](1+k_a[S]}$. For each curve, data given are [Py] in mol L^{-1}: ●, 1.12; ×, 2.25; ◑, 3.38; ○, 4.5; ⦶, 5.6; ◒, 6.76.

the intercept of the plot would give the value of the constant K_a. The related data in this experiments were plotted accordingly, gave a reasonable straight line (Fig. 11), and the calculated K_a value is 0.615. The full range of kinetic data corresponding to Figure 7 (at fixed [Py–SO_2] and different [Bz_2O_2] and [S] were then graphically plotted with the help of eq. (13), and the plots are given in Figure 12.

An interesting pattern is revealed by the plots in Figure 12. Under all conditions of [S] or [M] in either treatment, the experimental point on each plot falls reasonably on a straight line with zero slope if the mole ratio of [Bz_2O_2] : [Py–SO_2] $\geq$ 1, indicating exclusive bimolecular termination. However, altogether different kinetic patterns are revealed in each figure when the mole ratio of [Bz_2O_2] : [Py–SO_2] $\leq$ 1. For each dilution level with pyridine [S], the experimental points now fall on separate straight lines, each with a significant negative slope. A prominent degradative initiator transfer with little reinitiation is thus clearly indicated, with the respective effect being more prominent at a lower concentration than at a higher concentration of the rate-enhancing solvent pyridine, as revealed by the slope of the plots in the figure.

REFERENCES

1. P. Ghosh and S. Chakraborty, *Eur. Polym. J.,* **15,** 137 (1979).
2. P. Ghosh, S. Jana, and S. Biswas, *Eur. Polym. J.,* **16,** 89 (1980).
3. P. Ghosh, P. S. Mitra, and A. N. Banerjee, *J. Polym. Sci., Polym. Chem. Ed.,* **12,** 375 (1974).
4. P. Ghosh, A. R. Mukherjee, and S. R. Palit, *J. Polym. Sci.,* **A2,** 2807 (1964).
5. B. C. Mitra, P. Ghosh, S. R. Palit, *Makromol. Chem.,* **98,** 285 (1964).
6. P. Ghosh, A. N. Banerjee, *J. Polym. Sci., Polym. Chem. Ed.,* **12,** 375 (1974).
7. T. G. Fox, J. B. Kinsinger, H. F. Mason, and E. M. Shuele, *Polymer,* **3,** 71 (1962).
8. P. Ghosh and G. Mukherjee, *J. Polym. Sci., Polym. Chem. Ed.,* **12,** 375 (1974).
9. P. Ghosh, S. C. Chadha, A. R. Mukherjee, and S. R. Palit, *J. Polym. Sci.,* **A2,** 4433 (1964).
10. P. Ghosh, S. Chakraborty, and S. Biswas, *Makromol. Chem.,* **181,** 1331 (1980).